2010

Background estimation in MXGS apparatus on international space station

Behcet Alpat
INFN Sezione di Perugia Italy

Mauro Menichelli
INFN Sezione di Perugia Italy

Diego Caraffini
MAPRAD S.r.l., Italy

Marco Petasecca
University ofWollongong, marcop@uow.edu.au

Francesca Renzi
MAPRAD S.r.l., Italy

Background Estimation in MXGS Apparatus on International Space Station

Behcet Alpat, *Member, IEEE*, Mauro Menichelli, *Member, IEEE*, Diego Caraffini, Marco Petasecca, *Member, IEEE*, and Francesca Renzi

***Abstract*—This paper describes a study of background estimation in Modular x and gamma-ray Sensor (MXGS) on-board ESA's Atmosphere-Space Interactions Monitor (ASIM) mission, using Geant4 simulations and SPENVIS packages for particle flux generations.**

***Index Terms*—Environmental radiation effects, Monte Carlo background estimation, semiconductor device radiation effects, space station based experiment.**

I. Introduction

THE Atmosphere-Space Interactions Monitor (ASIM) [1] is an ESA science instrument assembly, to be installed on the Columbus External Platform Facility (CEPF) of the ISS (International Space Station), to study the giant electrical discharges (lightning) in the high-altitude atmosphere above thunderstorms. The discharges are seen as optical, X and gamma-ray flashes in the stratosphere and mesosphere. The optical emissions are dubbed *red sprites*, *blue jets*, and *elves* or, collectively, Transient Luminous Events (TLEs); the X and gamma-ray emissions are dubbed Terrestrial Gamma Ray Flashes (TGFs), instead. The ASIM mission comprises, therefore, two main scientific instruments: the Miniature Multi-spectral Imaging Array (MMIA) composed of six cameras and six photometers and the Modular X and Gamma-ray Sensor (MXGS).

We present the results obtained from Geant4 [2] simulation programs developed for the purpose of studying the background generated by charged cosmic-ray interactions in MXGS.

This work was divided in two phases. The simulation for the first stage (Phase I) was performed considering MXGS in open space and only the background due to prompt events was estimated. In the second phase (Phase II) MXGS was considered as attached to the ISS, so the geometry includes the structures surrounding the detector, to account for their modulating effect on the incident fluxes, and delayed background events due to activation were also taken into account. Since Phase II is more representative of the actual MXGS operating condition, in this paper we report its results only, although we give a description of both phases.

Manuscript received September 11, 2009; revised December 16, 2009; accepted January 22, 2010. Date of current version August 18, 2010.

B. Alpat and M. Menichelli are with the INFN Sezione di Perugia, 06123 Perugia (PG), Italy (e-mail: behcet.alpat@pg.infn.it; mauro.menichelli@pg.infn.it).

D. Caraffini and F. Renzi are with the MAPRAD S.r.l., 06127 Perugia, Italy (e-mail: diego.caraffini@maprad.com; francesca.renzi@maprad.com).

M. Petasecca is with the MAPRAD S.r.l., 06127 Perugia, Italy, and also with the University of Wollongong, Centre for Medical Radiation Physics, 2500 NSW, Australia (e-mail: marco.petasecca@maprad.com).

Color versions of one or more of the figures in this paper are available online at http://ieeexplore.ieee.org.

Digital Object Identifier 10.1109/TNS.2010.2042070

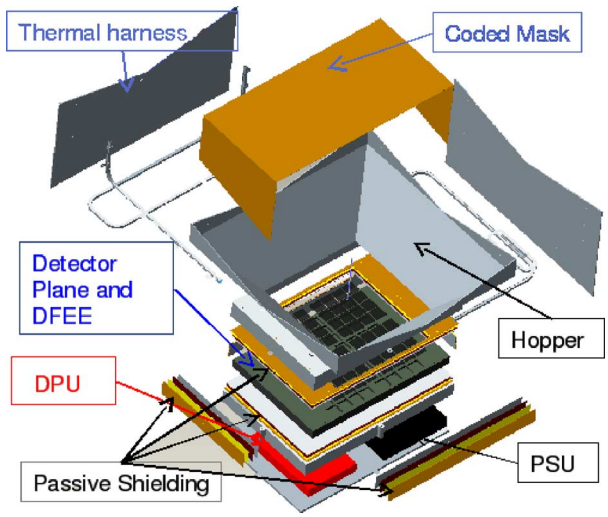

Fig. 1. Technical drawing of MXGS apparatus, MLI foils and crystals are not shown, but the holders which house each Cd–Zn–Te crystal are visible in detector plane. The holes in coded mask are not drawn.

II. MXGS Apparatus

The technical drawing of MXGS apparatus is shown in Fig. 1. The detector array is composed of 64 CdZnTe crystals of each of dimensions 4.0 cm × 4.0 cm × 0.5 cm, therefore its total sensitive area consists of a 1024 cm^2 plane. It is protected against the background radiation by a passive graded shield, surrounding the detector housing. This shield is formed by a stack of four layers, from inside to outside: 1 mm stainless steel, 0.5 mm Sn, 0.25 mm Ta and, finally, 2 mm of Pb. This graded configuration was used also in the Low Energy Gamma Ray Imager (LEGRI) instrument [3]. A hopper shaped collimator defines the 80° × 80° field of view for MXGS and shields the detector plane against the cosmic X-ray background. The Detector Front End Electronics (DFEE) is mounted in the housing below the detectors. The electronics comprise the PSU (HVPS/LVPS) module and the MXGS Data Processing Unit (DPU). A coded mask with a 50% open factor is mounted on top of the instrument. The MXGS apparatus is thermally isolated by two radiators and the areas not protected with radiators are covered with Multi Layer Insulator (MLI).

All parts previously described are modelled in Geant4, the geometry includes 74 different volumes and more than 10 different materials are defined. Fig. 2 shows the Geant4 geometry, the coded mask with a 50% open factor is clearly seen on top of the

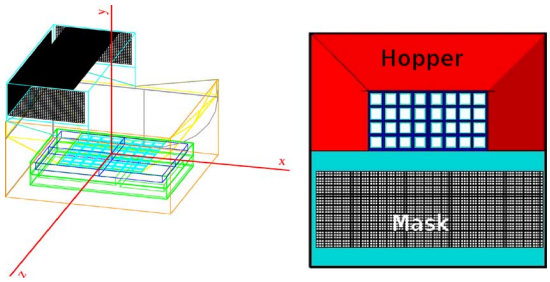

Fig. 2. Graphical renditions of the MXGS, generated by Geant4, based on the simulation geometry definitions. On the left, the wire-frame of MXGS is shown. On the right, the top view of apparatus shows coded mask and its holes (bottom half), hopper (around upper half), and detector plane with crystals.

instrument, other structures such as the detector housing, DPU, PSU and the entire plane of crystals are visible in the wire-frame version.

III. Preliminary Background Evaluation and Methodology Definition (Phase I)

The objectives of Phase I of this work were the implementation of the geometry of MXGS apparatus and the simulation of the main background sources in order to give a first assessment of ASIM/MXGS background performance, to validate our method and as a useful feedback for detector designers. In this phase only the prompt interactions of the following particles were used for background calculations:

- trapped protons and electrons (according to AP-8 MAX and AE-8 MAX models respectively);
- solar protons (according to JPL-91 model);
- cosmic protons and helium nuclei (according to CREME86, $\mathrm{M} = 1$ conditions);
- diffuse cosmic X-rays.

As shown in Fig. 3, the fluxes of galactic cosmic ions heavier than He are about two orders of magnitude smaller than the latter's. We expect that the main contribution to background rate is given by secondaries created by ionization (mostly electrons) and we assume their number to be roughly proportional to the square of the primaries' atomic number. Averaging all the species shown in the plot (heavier than He) and scaling to their nominal fluxes, we estimate that their total contribution is less than Helium (at most 70%), so we started considering only galactic cosmic H and Helium (similar approaches can be found in literature, for instance see [4]).

The differential fluxes are averaged over the three years of the ASIM mission (start date: January 1, 2011) at solar maximum and, with the exception of the diffuse cosmic X-rays one, were generated using SPENVIS [5]. To generate the diffuse cosmic X-ray background (CXB) instead, we used the following parameterization [6]:

$$f(E) = \frac{7.9\, e^{(-E/41.13)}}{E^{+1.29}} \rightarrow E < 60 \text{ keV}$$
$$f(E) = \frac{1652.0}{E^{+3.0}} + \frac{1.75}{E^{+1.7}} \rightarrow E > 60 \text{ keV} \qquad (1)$$

where $\mathrm{f(E)} * \mathrm{E}$ gives the CXB flux. We decided to use this parameterization, although other similar ones can be found in literature [7]. See also [8], which reports parameterization coincident with the ones we use for energies below 60 keV.

Geant4 version 4.8.3 was used for all results presented in this paper. The physics configuration used is similar to several simulation works. For instance, the hadronic processes are comparable to what can be found in [9]. We used the Binary Cascade model for nucleon-nuclei reactions [10], where applicable, and pre-compound and LEP models are used, respectively, at energies below and above the cascade regime. Data-driven models are included in the simulation to account for neutrons produced by the primaries' interactions. For electromagnetic interactions we included Low-Energy models as for instance in [11]. A general description of the physics models of Geant4 can be found in [2].

The events were generated uniformly according to $\mathrm{Cos}(\theta)$ law over the surface of an imaginary box which includes the entire MXGS apparatus. The Geant4 General Particle Source (GPS) was used to generate primary particle fluxes following a given spectrum.

The primary or secondary particles which interact with the CdZnTe crystals were recorded along with their prompt energy depositions. In case the deposited energy was within the range from 10 to 500 keV, i.e., the sensitivity range of MXGS, it was counted as a background event. The expected background rate was then obtained as

$$\mathrm{BkgRate}\left(\frac{\mathrm{particles}}{\mathrm{cm}^2 \cdot \mathrm{s}}\right) = \sum \frac{\mathrm{BkgEvent}_i \cdot \mathrm{SF}_i}{A} \qquad (2)$$

where the summation is over all the involved species and A is the total active area of the CdZnTe crystals. The scaling factor, SF_i, is different for each particle specie and/or simulation run. It is directly related to the equivalent exposure time for each specific configuration.

The background rate variations along the orbit were also studied in detail for trapped protons and electrons. The simulation for one day of mission ($\sim$ 15.75 orbits) was carried out over 1437 points along the orbit trajectory (provided by SPENVIS), so that the time difference between subsequent positions corresponded to a 60 s exposure. For each point the background rate was evaluated using the method described above. The creation of a grid of points along the orbit allowed us to define the area where the background is too high for operating MXGS and exclude it from our calculations. Such area (loosely referred to as SAA region) has been defined in slightly different ways for protons and electrons. Fig. 4 shows the SAA region for protons.

We evaluated, for each orbit, the time the experiment will spend within exclusion areas and the corresponding fluencies due to protons and electrons. We finally evaluated the average background rate along the orbit, both including and excluding the SAA, for trapped proton and electrons.

In this phase, we also performed a study of the influence of the electronic box shielding on the background levels induced by electrons, both primary ones and those produced by helium interacting with the surrounding structures. To this purpose, the MXGS apparatus Geant4 geometry was modified by removing the passive shielding and new simulation runs were performed.

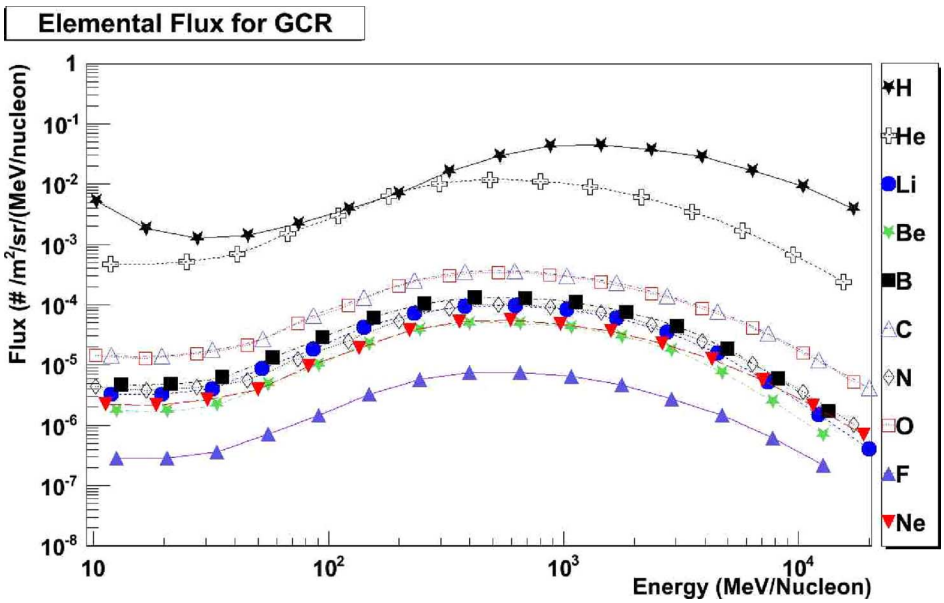

Fig. 3. Differential fluxes for several GCRs ion species as a function of their energy per nucleon created by SPENVIS. Flux values below 10 MeV/n are excluded from the plot since SPENVIS gave a flat spectrum in that region. We did not show the elements with fluxes lower than the ones present in the picture.

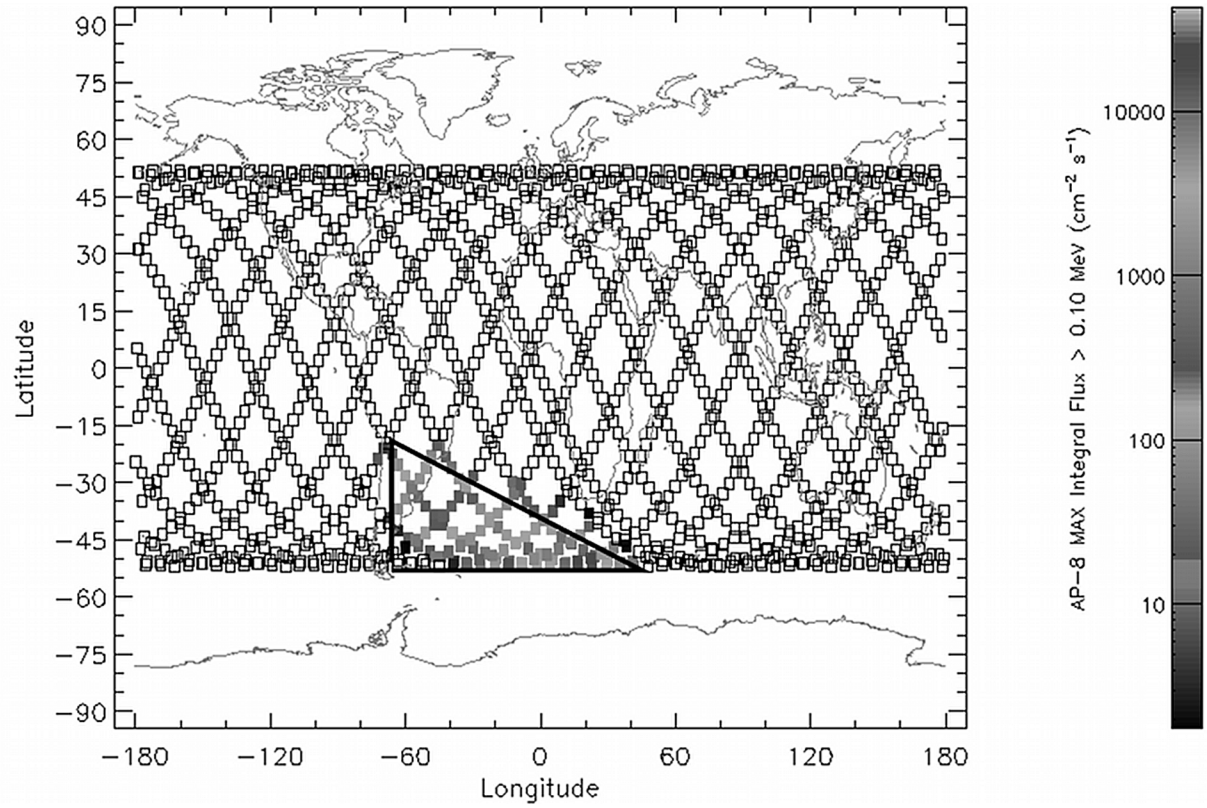

Fig. 4. Definition used by MAPRAD of SAA borders (thick line): it has been used to calculate the SAA included/excluded background rates for protons.

The results showed that background from primary electrons is significantly reduced by the presence of the shielding, while for the helium secondaries, the effect does not seem to be distinguishable, since most of them were produced inside the CdZnTe crystal holder, which is already inside the shielded volume.

IV. Background Evaluation Methodology and Simulation in Phase II

The Geant4 geometry implemented in the second part of the work, Phase II, is shown in Fig. 5. The big disk is the Geant4 model of Columbus. The larger box at the bottom is the ACES

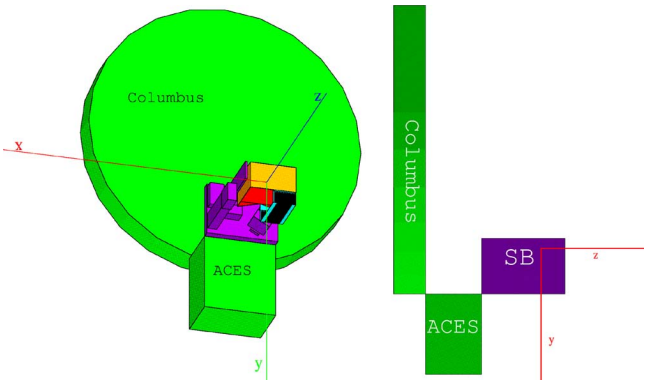

Fig. 5. On the left, GEANT4 view of the MXGS apparatus attached to the Columbus. On the right, side view of Geant4 geometry where ASIM is replaced with an enclosing box (SB) used to evaluate primary flux alteration by the presence of the supporting structures. The y axis is pointing towards the Nadir, the z axis is pointing towards open space.

instrument [12] and the remaining volumes are the other components of ASIM. All structures surrounding MXGS were modelled with much less details: there are 23 volumes of aluminium of such a thickness as to obtain the appropriate mass. About Columbus, we made the lateral dimension shorter than in reality, so that we could create a smaller surface of generation and therefore reduce the computing time. With this approximation, the particles could be shielded more than in the real situation. However, for all species except Galactic Cosmic Protons and Helium, Phase I results clearly showed that (even in absence of Columbus) the highest contribution to the background rate, is due to particles hitting the crystals from the one side not covered with passive graded shield ($y > 0$). We estimated that our approximation on Columbus shape affects the background rate due to GCR Protons and Helium at most by 10%.

The simulated background components included the atmospheric gamma-rays, besides those used in the Phase I.

Since the operating orbit goes through the polar and equatorial regions several times every day and the fluxes we used for all other species are averaged over long time tense, the parameterization employed to generate the atmospheric gamma-rays spectrum is the average of the following two functions [13]:

$$F_\gamma = 1.723 \cdot E^{-1.34} \text{ photon} \cdot \text{cm}^{-2} \cdot \text{s}^{-1} \cdot \text{keV}^{-1} \quad (3)$$

valid close the polar region, where average rigidity is about 3 GV and

$$F_\gamma = 0.539 \cdot E^{-1.39} \text{ photon} \cdot \text{cm}^{-2} \cdot \text{s}^{-1} \cdot \text{keV}^{-1} \quad (4)$$

valid near the equator, where average rigidity is 14.5 GV.

To further improve the efficiency in terms of computing time (about an order of magnitude by our estimates) and to account for the energy spectra deformation at MXGS surface caused by the interaction of Columbus and ACES with the incoming particles fluxes, we used the following approach. First, we generated a given number of events using the input flux (as given by SPENVIS) uniformly distributed over the surface of the Box of Generation, BG. Inside BG there were Columbus, ACES and a parallelepiped with the same dimensions of the Columbus External Platform Facility (CEPF, the box on the right side of Fig. 5, small box, or SB, in the following). The center of BG was located at the center of MXGS.

Subsequently, the differential fluxes of particles, reaching each face of the SB, was normalized to the one face looking to the open space which is alteration free, as we verified *a posteriori*. This was done also for the differential fluxes of secondary particles created by the interaction of primaries with the surrounding material. The corrected fluxes were used for the generation according to $\text{Cos}(\theta)$ law over a new box. In point of fact, this new box of generation is SB itself, with MXGS and the other components of ASIM set inside it. Since the distortion introduced by Columbus and ACES on energy spectra was different for each face of the new box of generation, as exemplified in Fig. 6, we had to treat each face separately when evaluating their contributions to the background, since equal numbers of generated particles would correspond to different exposure times for each face, leading to different scaling factors in accord to the formula:

$$t_i = \frac{A_i \cdot I_i}{G_i}. \quad (5)$$

Here, t_i is the equivalent exposure time for the i^{th} surface, A_i is the corresponding surface area, G_i is the number of particles generated and I_i is the integral of the particle's flux for the considered face.

The particles that interacted with the CdZnTe crystals were recorded along with their energy deposition. When the total energy deposited in each crystal by one particle was within the sensitivity range of MXGS, it was counted as background event. In this stage of the work, the evaluation of deposited energy was performed in a different and more accurate way in comparison to that in Phase I. In fact, in Phase II:

- the energies deposited in different crystals were considered as separate signals;
- for each (primary or secondary) particle P coming in one crystal, the total deposited energy was calculated as the sum of the energy deposited directly by P plus the energy deposited by the particles that P created in the same crystal. (In Phase I, the energy deposited by particles born in the crystal was not added to the energy deposited by their parent: each child was accounted for separately.)

The background rate variations along the orbit were also studied in detail for trapped protons and electrons; the approach we used was the same as for Phase I. Table I lists the fluencies for trapped protons and electrons on an orbit by orbit basis. The total time the experiment will spend inside SAA, evaluated according to our definition for trapped electrons is about three hours, while using the definition obtained from proton data, we find it to be slightly less than two hours. Table II summarizes the average background rate results.

Since we generated differential fluxes averaged over the three years of ASIM mission at maximum solar activity, the values in Table II are not the average count rate over an event. Most likely, during intense events, the data taken by ASIM will have to be rejected, (similarly to what happens in the SAA) when the count rate rises over some threshold.

The most important contributions are those due to trapped electrons. The diffuse X-rays, contribution, without taking into

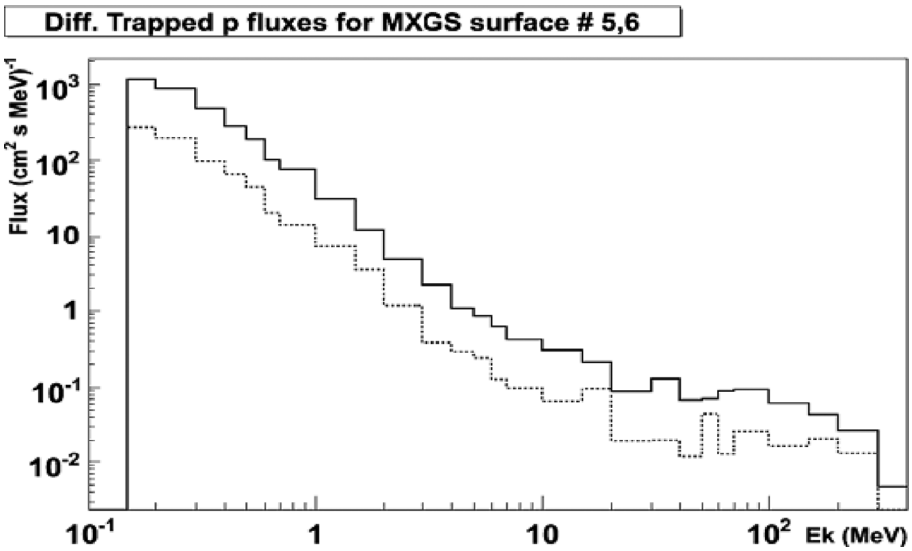

Fig. 6. Trapped proton differential fluxes generated on surface #5 (solid line) which is looking to open space and on surface #6 (dashed line) looking towards Columbus. Surface #5 and surface #6 are the faces of SB at $z > 0$ and $z < 0$ respectively.

TABLE I
FLUENCES IN SUCCESSIVE PASSAGES THROUGH THE SAA

Orbit number	Trapped Protons		Trapped Electrons	
	Passage Time	Fluence E>100keV	Passage Time	Fluence E>40keV
2	660	980727	1140	525326000
3	1140	4,63E+006	1740	1,16E+009
4	1320	4,01E+006	1560	1,02E+009
5	959,998	477528	1260	378296000
6	539,999	41864	719,999	627583000
7	480	37408,1	599,999	856182000
8	479,999	115577	539,999	727603000
9	419,999	52020,9	479,999	15872200
10	59,9998	457,259	300	14986,3
11	0	0	0	0
12	0	0	60,0003	8020,84
13	0	0	359,999	23263000
14	0	0	419,999	98610900
15	0	0	719,997	108552000
Total	**6059,9948**	**10348782**	**9899,9913**	**5,538E+09**

Fluence received by MXGS in successive passages through the SAA: for each orbit the time elapsed in the SAA area, as well as the fluence relative to two threshold values specific for each particle type.

TABLE II
AVERAGE BACKGROUND RATES

Particle Type	Total Background (cnts/cm^2·s)
Trapped protons	5.8
Trapped protons excluding SAA	0.06
Trapped electrons	7400.0
Trapped electrons excluding SAA	0.05
Solar protons	0.12
Atmospheric gamma-rays	1.5
GCR protons	0.26
GCR He	0.043

The background rates calculated using data averaged over the orbit of a day (1437 points (every point about 60 seconds)), for SAA both included and excluded. The fluxes used for the calculation are averages over the three years of ASIM' mission.

account the Earth shadowing is 25 cnt/$(\mathrm{cm}^2 \cdot \mathrm{s})$, but this drops down to 0.06 cnt/$(\mathrm{cm}^2 \cdot \mathrm{s})$ when the Earth shadowing is present in ASIM's FOV, as it will be in the real case. The electrons are mostly localized around the SAA and magnetic pole areas and could be reduced greatly if such areas were to be excluded from data taking.

In the last phase of this work we estimated the delayed background rate. When the particles will hit MXGS during its mission, they could produce nuclear interactions, creating unstable isotopes within the apparatus. This will mainly happen inside SAA, where the trapped proton flux rises to its maximum, but the decay products will affect the background rate at a successive time. To evaluate this source of background we performed a specific simulation run, generating 15 million protons at the surface SB, with the average spectrum of trapped component. Other possible sources were not considered such as Galactic Cosmic Ray protons and helium nuclei, although their capacity to activate the material is higher, since their flux is much smaller than the trapped proton one. The 15 million generated protons provided a total of 5147 decays which released a relevant signal in the CdZnTe crystals, considering the observation range and also the dead time of the apparatus. Such decays will affect a very long time span, that covers the whole three years of the MXGS mission and more, but the overwhelming majority takes place in relatively short time after the activation itself. For our study we did not separate the involved species of radioactive isotope, but we considered the overall distribution of the decay time (shown in Fig. 7) as the result of a short exposure to the average trapped proton flux and we used it to evaluate the corresponding decay rate.

We did this for a time span of one year, shorter than the whole mission duration, since by that time and at later ones we expected to reach a somewhat stable level in the induced background. Such distribution is essentially the decay rate as a function of time since the exposure to the average cosmic fluxes: to reproduce the effect such exposure at a given location (time) along the orbit has on subsequent ones, we only had to scale the histogram by a normalization factor (NormFactor) in accordance to the flux distributions given by SPENVIS for each orbit position. Thus, we were able to determine the contribution of

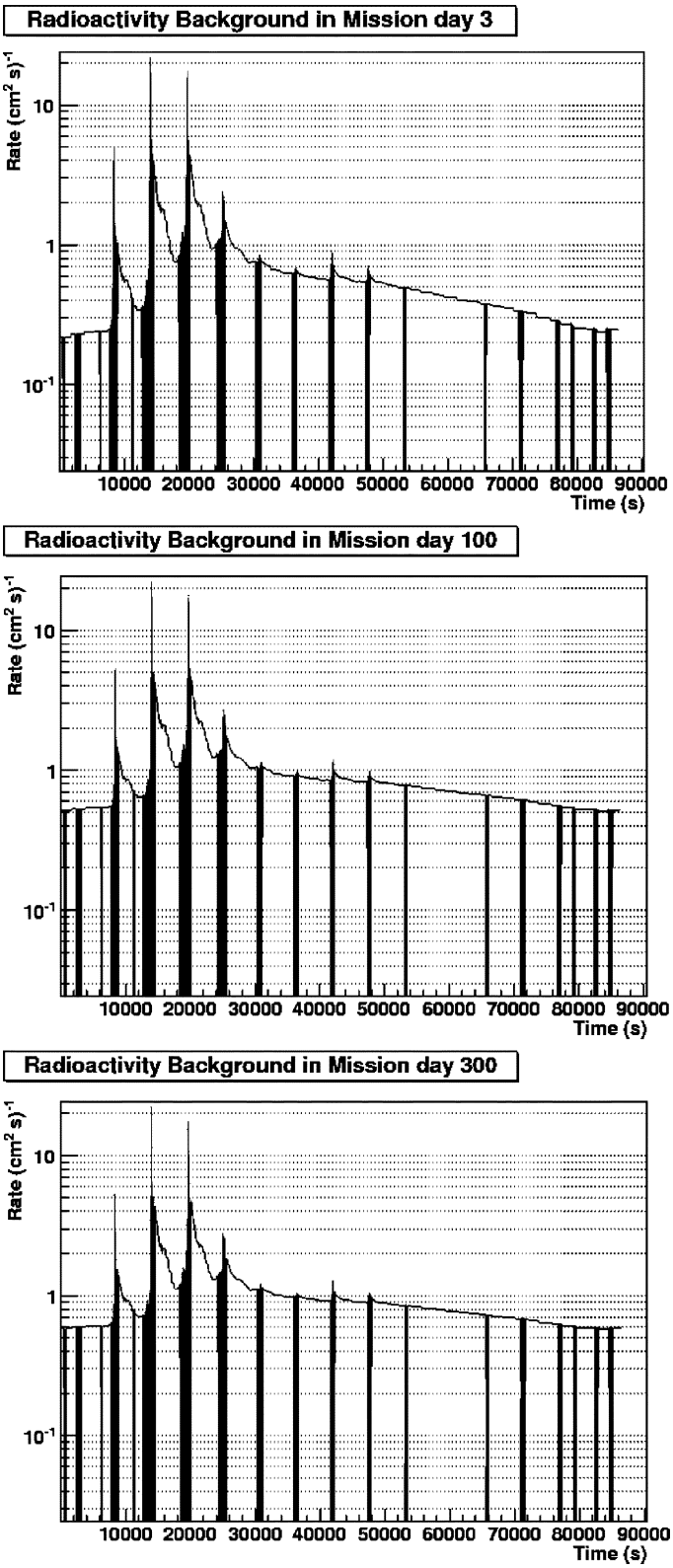

Fig. 7. Expected activation background for mission day 3, day 100, day 300: the Euro filled areas refer to time spent in SAA or otherwise high flux areas; empty line refers to the outside.

the exposure at each orbit point to the activation background as a function of time after the exposure itself.

With this result in hand we could obtain the total decay rate at any given orbital position, corresponding to time T, by summing

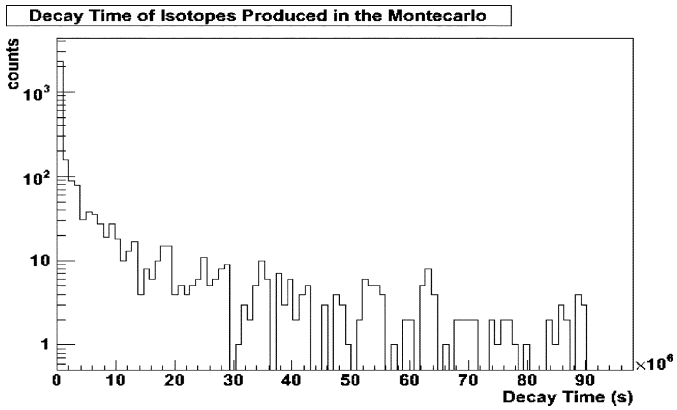

Fig. 8. Distribution of the decay time of nuclei produced in the Geant4: the x axis spans three years.

the contribution from every previous one (time t), according to the formula:

$$\mathrm{TotalRate}_T = \sum \mathrm{NormFactor}_{\,t} \cdot \mathrm{Rate}_{T-t} \tag{6}$$

where $\mathrm{Rate}_{T\text{-}t}$ is the rate evaluated from the histogram in Fig. 6, considering as decay time the difference $T-t$ between the current time and the one of the contributing position. Using this approach we were able to evaluate the expected background level due to activation for any mission day of our choice in the first year. In Fig. 8 the evaluated level is shown as a function of time within the day 3, day 100, and day 300 of the mission. The plot for day 100, corresponding to about three months, displays higher values than the one for day 3, due to pileup effect, but from then on to the end of the first year of mission (day 300) there is no significant variation, since the creation rate of new nuclei equals the decay rate (secular equilibrium). The plots for day 100 or day 300 are therefore representative of a near-equilibrium situation.

V. Conclusion

In this paper, we described our Monte Carlo approach to the estimation of the Cosmic-ray induced background counting rate of the MXGS apparatus, which will be installed on the ISS as part of the ASIM experiment. We used SPENVIS to evaluate the particle fluxes expected in the orbital environment and Geant4 to assess their effects on the detector.

The main results we achieved are as follows:

- the evaluation of the prompt background rate given by averaged cosmic ray fluxes;
- the evaluation and subtraction of the contribution to the average due to the SAA region and evaluation of the corresponding passage (dead) time;
- the evaluation of the background as a function of time (on a daily basis), induced by activation of the CdZnTe sensor, as well as that of the materials which compose MXGS and its surrounding structures.

After exclusion of the SAA region, the prompt background rate is 2.09 $\mathrm{cnt}/(\mathrm{cm}^2\mathrm{s})$, whereas the delayed background rate produces a comparable contribution (SAA excluded). This result is compatible with the background level observed in the LEGRI experiment which used a similar sensor system [3]. As noted in

Section II the inclusion of heavier Galactic Cosmic Nuclei can give contribution comparable to Helium (0.043 cnt$/(\mathrm{cm}^2\mathrm{s})$), which is about 2% of evaluated prompt background rate.

This approach was developed to study the background of a detector, but it can be applied, for instance, to the accurate evaluation of LET spectra on VLSI circuits operating in Earth orbit, taking into account the shielding effect of the surrounding materials, using the actual configuration of the apparatus.

ACKNOWLEDGMENT

The authors greatly appreciated the support of the ASIM collaboration; in particular we thank Prof. V. Reglero and Dr. J. M. Rodrigo. The authors are also grateful to Prof. C. Budtz-Jørgensen and Dr. I. Kuvvetli for their helpful comments during the preparation of this work.

REFERENCES

[1] ASIM, Atmosphere-Space Interactions Monitor. [Online]. Available: http://www.space.dtu.dk/English/Research/Projects/ASIM.aspx

[2] Geant4 a Toolkit for the Simulation of the Passage of Particles Through Matter. [Online]. Available: http://geant4.web.cern.ch/geant4/

[3] F. Sanchez *et al.*, "Background in low Earth orbits measured by LEGRI telescope-short and long term variability," *Nucl. Instrum. Methods Phys. Res. B*, vol. 155, no. 1, 2, pp. 160–168, 1999.

[4] A. J. Dean *et al.*, "Background in space-borne low-energy γ ray telescope," *Space Sci. Rev.*, vol. 57, pp. 109–186, 1991.

[5] SPENVIS, Space Environment Information System [Online]. Available: http://www.spenvis.oma.be/

[6] V. Reglero, internal document, Astronomy and Space Science Group, Instituto de Ciencia de los Materiales, Universidad de Valencia, Spain, ASIM-UV-MXGS-REQ-001; Rev: 1.0.

[7] D. E. Gruber, J. L. Matteson, L. E. Peterson, and G. V. Jung, "The spectrum of diffuse cosmic hard X-rays measured with HEAO-1," *Astrophys. J.*, vol. 520, pt. 1, pp. 124–129, 1999.

[8] F. Frontera *et al.*, "The cosmic X-Ray background and the population of the most heavily obscured AGNs," 2007 [Online]. Available: arXiv:astroastro-ph/0611228v2

[9] T. Ersmark *et al.*, "Geant4 Monte Carlo simulation of belt proton radiation environment on board the International Space Station/Columbus," *IEEE Trans. Nucl. Sci.*, vol. 54, no. 4, pp. 1444–1453, 2007.

[10] G. Folger *et al.*, "The binary cascade-nucleon nuclear reactions," *Eur. Phys J. A*, vol. 21, pp. 407–417, 2004.

[11] C. Tenzer *et al.*, "Monte Carlo simulations of stacked X-ray detectors as designed for SIMBOL-X," in *Proc. SPIE*, 2006, vol. 6266, pp. 6266–97.

[12] ACES Atomic Clock Ensemble in Space. [Online]. Available: http://www.spaceflight.esa.int/projects/index.cfm?act=default.page&level=12&page=829

[13] A. J. Dean *et al.*, "The gamma ray emissivity of Earth's atmosphere," *Astron. Astrophys.*, vol. 219, pp. 358–361, 1989.